Precise localization and correlation of single nanoparticle optical responses and morphology

Rongchao Jin, Justin E. Jureller, and Norbert F. Scherer[a)]
Department of Chemistry, James Franck Institute, and Consortium for Nanoscience Research, The University of Chicago, 5735 South Ellis Avenue, Chicago, Illinois 60637

(Received 31 October 2005; accepted 3 May 2006; published online 28 June 2006)

We demonstrate nanometer scale localization of the nonlinear optical response of single nanoparticles and aggregates and correlate this with their morphology. The essence of our approach is to create position markers on an optical and electron-transparent substrate (Si_3N_4 thin film) that allows optical measurements and transmission electron microscopy (TEM) imaging of the identical nanoparticles or aggregates. The second harmonic activity optical image of individual Ag nanostructures is registered with the TEM image. Centroid localization of the optical signals allows correlation with better than 25 nm precision. This is sufficient to determine the origin of optical "hot spots" within multiparticle aggregates. © *2006 American Institute of Physics*.
[DOI: 10.1063/1.2213518]

Understanding the structure-property relationship of nanoparticles and tailoring their optical and electronic properties are prerequisites to designing functional nanomaterials.[1] "Bottom-up" fabrication of materials based upon nanoscale building blocks (nanoparticles or nanocrystals) is being extensively pursued.[2–8] The dimensions of nanocrystals (typically 2–100 nm) lie between bulk crystals and single molecules. Electron confinement effects give the nanocrystals unique properties that are fundamentally different from their bulk or atomic cluster counterparts.[8–10]

The linear and nonlinear optical properties of metal and semiconductor nanocrystals are of particular interest for optical and biosensing applications.[11,12] Most previous studies examined bulk properties of nanoparticle solutions, such as linear scattering, absorption and second harmonic (SH) generation (SHG).[3,4,13–15] These ensemble measurements provide information averaged over the nanoparticle size and morphology distributions, and thus, the precise structure-property relationship of individual nanoparticles is obscured. Therefore, single-particle measurements are necessary to gain a deep and complete understanding of their optical properties and those of individual particle aggregates.[16–23]

In optical microscopy-based single-particle measurements, the diffraction limit prevents the morphology of single nanoparticles from being revealed.[16] Although one might identify single nanoparticles by scrutinizing their optical signatures (e.g., linear scattering spectra), in some cases, this may not be sufficient due to similarity of optical signatures of different nanostructures; e.g., both nanorods and nanoparticle dimers can exhibit transverse and longitudinal plasmon modes at similar wavelengths;[4,10,24] therefore, resolving the fine structure of the nanoparticles requires joint analysis with nanoscale imaging. Near-field optical microscopy[25] extends the optical and topographic resolution to ~50 nm but involves a complicated excitation field, including tip-sample optical (plasmon) interactions.[22] Atomic force microscopy (AFM) allows *in situ* imaging and correlation with optical measurements,[26–28] but still with limited lateral resolution (1–5 nm) and nontrivial tip-sample convolution. Transmission electron microscopy (TEM) has significantly higher resolution (0.1 nm) than AFM or scanning electron microscopy (SEM) and also allows elemental and structural analyses on the subnanometer scale. Therefore, integrating optical measurements and TEM imaging would be a powerful way to precisely correlate the structure-property relationship in nanomaterials.

This letter reports a facile methodology for correlating optical measurements and TEM imaging of identical nanoparticles or multiparticle aggregates in pursuit of a precise structure-function relationship. The essence of our approach is to create position markers on an optical and electron-transparent substrate (e.g., Si_3N_4 thin film). This permits *ex situ* correlation of optical and TEM images. The utility is demonstrated by correlating optical SH activity of single Ag nanoparticles and their precise structure imaged by TEM.

The substrate is a Si_3N_4 thin film window (0.2×0.2 mm^2, film thickness ~100 nm) supported on a silicon wafer (~3 mm diameter, ~0.2 mm thickness) (SPI Supplies). The position markers were fabricated by electron-beam lithography using PMMA as a resist (Fig. 1). Two sizes of position markers were fabricated [Fig. 2(a)]: micron scale bars (0.75×7.5 μm^2) and nanometer scale dots (~100 nm diameter). The bar markers allow one to easily identify the imaged area in both optical microscopy and TEM analysis, as well as coarse superposition of the two images. The nanodot markers permit precise registration of the optical signals with the high-resolution TEM images.

The PMMA pattern was translated into metal markers by thermal evaporation of a 30 nm thick Cr or Ag film onto the

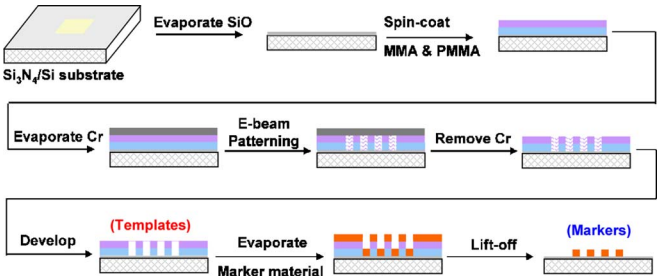

FIG. 1. (Color online) Fabrication of position markers on a Si_3N_4 window (100 nm thick). See text for further explanation.

[a)]Author to whom correspondence should be addressed; electronic mail: nfschere@uchicago.edu

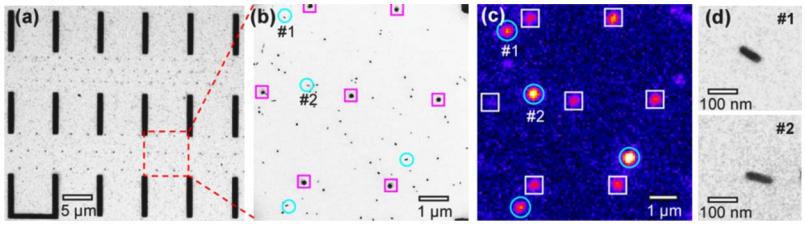

FIG. 2. (Color online) (a) TEM image of a position marker pattern consisting of bars and nanodots. (b) 5× magnified view of a region in (a). (c) SH optical image (false color image) of the same area as (b). The circled spots in (b) and (c) are single Ag nanorods giving SH signals. The spots marked by squares forming a hexagonal pattern are the dot markers (~100 nm diameter). (d) Zoom-in images of single nanorods (1 and 2) shown in image (b).

substrate. Finally, the substrate was soaked in acetone at RT for ~15 min to lift off the polymer/metal film. The substrate was further coated with a layer of positively charged poly-(diallyldimethylammonium chloride) (PDDA, low molecular weight, Aldrich) to enhance the Ag nanoparticle adhesion to the substrate surface. In a typical experiment, the Si_3N_4/SiO window was immersed in a 0.2 wt % PDDA aqueous solution for several hours, allowing deposition of a layer of PDDA polymer on the window surface. The substrate was rinsed with water and dried. The roughness of the final substrate is ~0.5 nm (rms).

Ag nanoparticles were synthesized by citrate reduction.[10] A 5 ul aliquot of the Ag colloidal solution (1:4 diluted with water) was pipetted onto the window, allowed to stand for 5–10 min for nanoparticle deposition via electrostatic interaction (the Ag nanoparticles are negatively charged), then rinsed with water and dried. TEM imaging of the marked window area was carried out with a Tecnai F30 TEM equipped with a Schottky field emission gun.

Figure 2(a) shows a TEM image of a typical position marker pattern consisting of bars and nanodots. A zoomed-in area is shown in Fig. 2(b). Figure 3 compares the AFM and TEM images of an identical area. Due to tip-sample convolution, AFM cannot resolve fine structures and interparticle gaps revealed by TEM.

The Si_3N_4 window substrate with position markers can be used in absorption, scattering, and nonlinear optical measurements. This letter demonstrates correlation and localization of optical SH activity of single Ag nanoparticles or aggregates and their precise structure imaged by TEM. The SH activity map [e.g., Fig. 2(c)] was acquired with a homebuilt nonlinear optical microscopy system consisting of an inverted microscope (Nikon TE2000) and a tunable femtosecond pulsed Ti:sapphire laser source (Spectra Physics Mai-Tai broadband) described elsewhere.[10]

Prior to the SHG measurements, a bright field image of the marked area of the sample was acquired with white light illumination from a halogen lamp. The sample position was mechanically fixed and the femtosecond pulses were then introduced. Careful adjustment of the focal plane ensured an optimized SH signal from the Ag nanoparticles. Epi-scattered SH signals were collected. Figure 2(c) shows the SH image of Ag nanoparticles for the identical area as in Fig. 2(b). Emission spectra, laser polarization, and excitation wavelength dependence confirmed that the detected signals are SH activity and not two-photon fluorescence.[10] Nanoparticles with a nonspherical shape (e.g., Ag nanorods) exhibit much greater SH activity than isolated single quasispherical nanoparticles [Fig. 2(d)]. The direct and precise correlation of the structure and SH activity (and other spectral properties[10]) allow concluding that the SH signal from the highly active Ag nanostructures (i.e., nanorods, touching dimers, and clusters) arises from a mechanism of one-photon resonant excitation of the longitudinal plasmon mode of nanorods or dimers.[10] The plasmon excitation creates a nonlinearity, radiating harmonics (such as 2ω and 3ω) of the laser driving frequency (ω). This nonlinearity would be enhanced from the large local field associated with the longitudinal plasmon excitation,[9,29] which is significantly larger than that from the dipole plasmon of quasispherical particles.

For multiparticle (aggregate) structures, an important fundamental issue is to localize the SH emission site(s) within the aggregate. Previous research has reported different types of optically active (fractal) nanostructures,[30–33] however, lacking sufficient structural information and image-structure correlation to allow accurate electrodynamic simulation. Our methodology allows facile and precise determination of the SH emission site within an aggregate structure. We register the SH optical micrograph and TEM image with a linear mathematical transformation (image stretching and rotation, see supporting information) of the SH image [Fig. 4(a)]. The nanodot markers, visible in both the SH and TEM images, serve as reference points [the dots marked with squares in Fig. 4(a)] to determine the linear transform. The centroid of the optical point spread function is calculated for each reference marker. The signal-to-noise ratio (S/N) of the SH response typically allows this to be determined with <10 nm precision. Next, the centroids of SH emission spots [Fig. 4(a), red circles] for single Ag nanoparticles or individual aggregates are determined by a two dimensional Gaussian fit[34,35] and transformed into the TEM image frame [Fig. 4(a)]. The error of image correlation is estimated to be <25 nm.

Since aggregates exhibit multiple plasmon resonance bands in the visible and near infrared,[19,36] we investigated the SH activity of Ag nanoparticle aggregates for different excitation wavelengths [Figs. 4(b)–4(e)]. Aggregate 1 shows two emission centroids [red circles in Figs. 4(b) and 4(c)], one of which shifts as the excitation wavelength changes from 830 nm [Fig. 4(b)] to 880 nm [Fig. 4(c)], while the other essentially remains unshifted. For those small clusters [e.g., 2 in Figs. 4(d) and 4(e)], no distinct shift was observed

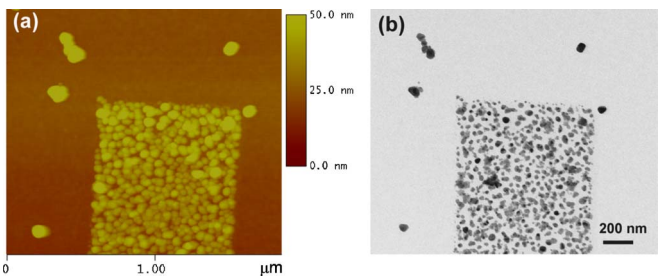

FIG. 3. (Color online) AFM and TEM images of a bar marker and nearby Ag nanoparticles.

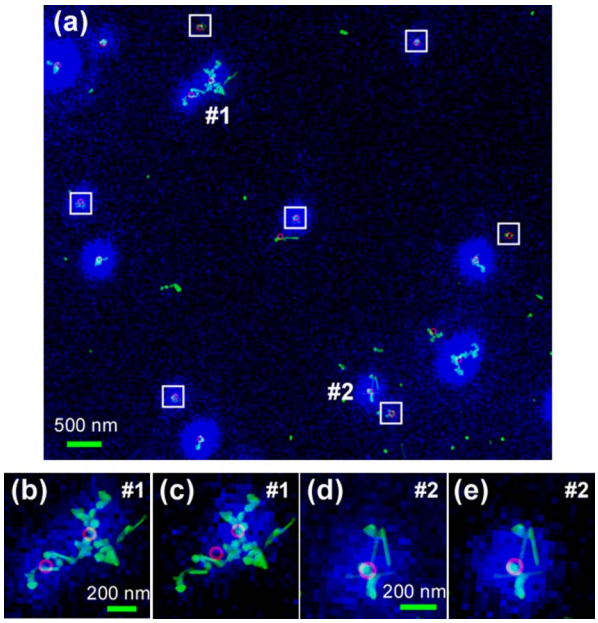

FIG. 4. (Color online) (a) Registered and colocalized SH optical and TEM images of an area (λ_{ex}=830 nm), blue: SH emission, red circles: the centroids of SH emission spots. The lithographically fabricated dots (marked with squares) serve as reference points for the image superimposition. (b)–(e) Centroid analysis of SH emission from multiparticle aggregates 1 and 2, (b) and (d): λ_{ex}=830 nm, (c) and (e): λ_{ex}=880 nm.

within the error. Higher-resolution TEM measurements allowed determining the precise structure of SH-active "hot" sites in relatively simple multiparticle aggregates, such as a SH-active cavity formed by three adjacent particles (see supporting Fig. S4). Wavelength-dependent data (not shown) point to a resonance enhancement mechanism[10] for the aggregates. The SH activity arises from the nonuniform polarization responses of the highly driven plasmon excitation.[37] The SH activity would also be enhanced from the large local field associated with the plasmon excitation within an aggregate structure, reminiscent of surface-enhanced Raman scattering.[38] We believe that the centroid shifting is related to the plasmon responses of the different spectral response of the various optical hot sites. Taken together, these results indicate that the nanoparticle aggregates have complex optical behavior due to their structural complexity, e.g., multiple optically active sites. Further work on the comparison of various linear and nonlinear optical behaviors, high-resolution structural characteristics of those SH-active sites in an aggregate, and theoretical modeling of the local field distribution is underway.

The methodology for correlating and localizing the optical response of single nanoparticles or aggregates and TEM imaging of particle morphology enables determining the origin of optical hot spots within multiparticle aggregates. This method is general and can be adapted for single-particle Rayleigh scattering, surface-enhanced Raman scattering (SERS), and ultrafast pump-probe studies.[39]

This work was supported by the NSF (CHE0317009), the University of Chicago MRSEC (DMR0213745), and the Consortium for Nanoscience Research. One of the authors (J.E.J.) acknowledges a Fellowship from the Burroughs-Wellcome Fund Interfaces Program (1001774). The authors thank H. Kim and Qiti Guo for experimental assistance.

[1] D. L. Feldheim and C. A. Foss, Jr., *Metal Nanoparticles: Synthesis, Characterization, and Applications* (Marcel Dekker, New York, 2002).
[2] M. A. El-Sayed, Acc. Chem. Res. **34**, 257 (2001).
[3] R. Jin, Y. Cao, C. A. Mirkin, K. L. Kelly, G. C. Schatz, and J. G. Zheng, Science **294**, 1901 (2001).
[4] M. Z. Liu and P. Guyot-Sionnest, J. Phys. Chem. B **108**, 5882 (2004).
[5] C. A. Foss, G. L. Hornyak, J. A. Stockert, and C. R. Martin, J. Phys. Chem. **98**, 2963 (1994).
[6] C. M. Lieber, Nano Lett. **2**, 81 (2002).
[7] C. P. Collier, T. Vossmeyer, and J. R. Heath, Annu. Rev. Phys. Chem. **49**, 371 (1998).
[8] M. G. Bawendi, M. L. Steigerwald, and L. E. Brus, Annu. Rev. Phys. Chem. **41**, 477 (1990).
[9] K. L. Kelly, E. Coronado, L. L. Zhao, and G. C. Schatz, J. Phys. Chem. B **107**, 668 (2003).
[10] R. Jin, J. E. Jureller, H. Y. Kim, and N. F. Scherer, J. Am. Chem. Soc. **127**, 12482 (2005).
[11] N. L. Rosi and C. A. Mirkin, Chem. Rev. (Washington, D.C.) **105**, 1547 (2005).
[12] J. J. Mock, M. Barbic, D. Smith, D. Schultz, and S. Schultz, J. Chem. Phys. **116**, 6755 (2002).
[13] C. Landes, M. Braun, and M. A. El-Sayed, Chem. Phys. Lett. **363**, 465 (2002).
[14] R. Antoine, P. F. Brevet, H. H. Girault, D. Bethell, and D. J. Schiffrin, Chem. Commun. (Cambridge), 1901 (1997).
[15] A. Brysch, G. Bour, R. Neuendorf, and U. Kreibig, Appl. Phys. B: Lasers Opt. **68**, 447 (1999).
[16] M. A. van Dijk, M. Lippitz, and M. Orrit, Acc. Chem. Res. **38**, 594 (2005).
[17] C. Sonnichsen and A. P. Alivisatos, Nano Lett. **5**, 301 (2005).
[18] S. Empedocles and M. Bawendi, Acc. Chem. Res. **32**, 389 (1999).
[19] J. Jiang, K. Bosnick, M. Maillard, and L. Brus, J. Phys. Chem. B **107**, 9964 (2003).
[20] M. Jacobsohn and U. Banin, J. Phys. Chem. B **104**, 1 (2000).
[21] R. D. Schaller, J. C. Johnson, K. R. Wilson, L. F. Lee, L. H. Haber, and R. J. Saykally, J. Phys. Chem. B **106**, 5143 (2002).
[22] S.-K. Eah, H. M. Jaeger, N. F. Scherer, G. P. Wiederrecht, and X.-M. Lin, J. Phys. Chem. B **109**, 11858 (2005).
[23] Y.-H. Liau and N. F. Scherer, Appl. Phys. Lett. **74**, 3966 (1999).
[24] T. Jensen, L. Kelly, A. Lazarides, and G. C. Schatz, J. Cluster Sci. **10**, 295 (1999).
[25] M. A. Paesler and P. J. Moyer, *Near-Field Optics: Theory, Instrumentation, and Applications* (Wiley, New York, 1996).
[26] W. E. Doering and S. Nie, J. Phys. Chem. B **106**, 311 (2002).
[27] J. Vasenka, C. Mosher, S. Schaus, L. Ambrosio, and E. Henderson, BioTechniques **19**, 240 (1995).
[28] L. A. Kolodny, D. M. Willard, L. L. Carillo, M. W. Nelson, and A. Van Orden, Anal. Chem. **73**, 1959 (2001).
[29] L. Gunnarsson, T. Rindzevicius, J. Prikulis, B. Kasemo, M. Kall, S. Zou, and G. C. Schatz, J. Phys. Chem. B **109**, 1079 (2005).
[30] R. J. Gehr and R. W. Boyd, Chem. Mater. **8**, 1807 (1996).
[31] M. I. Stockman, V. M. Shalaev, M. Moskovits, R. Botet, and T. F. George, Phys. Rev. B **46**, 2821 (1992).
[32] M. I. Stockman, D. J. Bergman, C. Anceau, S. Brasselet, and J. Zyss, Phys. Rev. Lett. **92**, 057402 (2004).
[33] M. J. Feldstein and N. F. Scherer, Proc. SPIE **3272**, 58 (1998).
[34] R. E. Thompson, D. R. Larson, and W. W. Webb, Biophys. J. **82**, 2775 (2002).
[35] X. Qu, D. Wu, L. Mets, and N. F. Scherer, Proc. Natl. Acad. Sci. U.S.A. **101**, 11298 (2004).
[36] T. J. Norman, Jr., C. D. Grant, D. Magana, J. Z. Zhang, J. Liu, D. Cao, F. Bridges, and A. Van Buuren, J. Phys. Chem. B **106**, 7005 (2002).
[37] J. I. Dadap, J. Shan, K. B. Eisenthal, and T. F. Heinz, Phys. Rev. Lett. **83**, 4045 (1999).
[38] G. C. Schatz and R. P. Van Duyne, in *Handbook of Vibrational Spectroscopy*, edited by J. M. Chalmers and P. R. Griffiths (Wiley, New York, 2002), pp. 759–774.
[39] See EPAPS Document No. E-APPLAB-88-293624 for supplemental information. The document may also be reached via the EPAPS homepage (httpL//www.aip.org/pubservs/epaps.html) or from ftp.aip.org in the directory /epaps. See the EPAPS homepage for more information.